Research Square

Preprints are preliminary reports that have not undergone peer review.
They should not be considered conclusive, used to inform clinical practice,
or referenced by the media as validated information.

Latent Behavior-Brain Dimension Reveals Heterogeneity in Attention-Deficit/Hyperactivity Disorder

Tingyong Feng

fengty0@swu.edu.cn

Southwest University https://orcid.org/0000-0001-9278-6474

Yao Yin

Southwest University

Ting Xu

Southwest University

Xueke Wang

Southwest University

Article

Keywords:

Posted Date: November 4th, 2026

DOI: https://doi.org/10.21203/rs.3.rs-11305701/v1

License: This work is licensed under a Creative Commons Attribution 4.0 International License.
Read Full License

Additional Declarations: The authors have declared there is **NO** conflict of interest to disclose

Abstract

To better capture the interindividual variability of Attention-deficit/hyperactivity disorder (ADHD), there is a growing need to shift research from categorical to dimensional approaches that integrate neuroscience with multiple behavioral domains. We applied multivariate partial least squares correlation (PLSC) to identify covariance patterns between behavioral domains (including clinical symptoms, neurocognitive impairments, and co-occurring mental and functioning conditions) and resting-state functional connectivity (RSFC) in children with ADHD. We further assessed the neurobiological relevance of the identified RSFC patterns. Finally, the predictive validity of the RSFC patterns for ADHD symptoms was tested in two independent cohorts. PLSC identified a single statistically significant latent dimension in the discovery sample, linking an RSFC pattern predominantly involving the ventral attention network (VAN) and somatomotor network (SMN) to an ADHD-related behavioral profile. This RSFC pattern showed significant spatial correspondence with the distribution of dopamine receptors, noradrenaline transporters, and serotonin transporters. Importantly, the RSFC pattern significantly predicted ADHD symptoms in both validation cohorts. We identified an RSFC pattern predominantly involving the VAN and SMN that is associated with multidomain ADHD-related behaviors, corresponds spatially to ADHD-related neurotransmitter distributions, and predicts ADHD symptom severity in independent samples. This pattern may serve as a candidate biomarker for future treatment targeting and treatment-response monitoring in ADHD.

Introduction

Attention-deficit/hyperactivity disorder (ADHD) is a common neurodevelopmental disorder with early onset, affecting approximately 4.8% – 5.9% of school-aged children and adolescents globally.[1–4] Individuals with ADHD often experience educational underachievement, occupational failure, poor socialization, and increased risk of accidental injuries, leading to significant economic burdens for individuals, families, and society.[5] However, personalized and effective treatments for ADHD are lacking due to the heterogeneity in symptom presentations (inattention, hyperactivity/impulsivity), neurocognitive impairments (e.g., inhibition, working memory, risk-taking propensity), co-occurring mental and functioning conditions (e.g., oppositional defiant disorder, conduct problems, social difficulties), and brain dysfunctions across individuals.[6] Previous studies that adopted the categorical approach or focused on a single ADHD domain fail to capture its heterogeneity.[7] Therefore, transitioning from categorical to dimensional approaches is essential for better understanding ADHD's heterogeneity. Dimensional methods can identify latent ADHD-related dimensions characterized by specific behavioral and brain functional features, which may facilitate clinical translation and ultimately improve prevention, diagnosis, treatment, and prognosis.

Dimensional approaches often rely on multivariate, data-driven statistical techniques, such as partial least squares correlation (PLSC) and canonical correlation analysis (CCA), to identify latent dimensions linking interindividual variability in brain structure or function with variability in behavioral measures.[8,9]

These approaches have been increasingly applied across psychiatric conditions, including major depressive disorder, autism spectrum disorder, and ADHD, revealing joint multivariate associations between brain and behavioral features.[7,10–14] In ADHD, dimensional studies have examined relationships between brain structure—such as cortical folding and white matter microstructure—and clinical/behavioral profiles including ADHD symptoms, emotional dysregulation, and prenatal alcohol exposure.[13,14] Other studies have linked brain function, including resting-state and dynamic functional connectivity, with ADHD behaviors or cognitive functions.[7,12] Nevertheless, few ADHD studies have simultaneously integrated ADHD symptoms, neurocognitive impairments, and co-occurring mental and functional conditions to explore their relationship with intrinsic brain functional connectivity, which is necessary to draw a more comprehensive picture of ADHD and improve its neurobiological validity.

Resting-state networks are typically derived from resting-state functional MRI (rs-fMRI) signals and are thought to reflect intrinsic brain functional connectivity.[8] Unlike task-based fMRI, rs-fMRI does not require participants to perform specific tasks, facilitating data acquisition and enabling its widespread use in ADHD research across all age groups. Over the past decade, ADHD has increasingly been conceptualized as a disorder of large-scale brain network dysfunction rather than alterations in single brain regions.[15,16] Converging evidence has linked aberrant resting-state functional connectivity (RSFC) of large-scale networks to clinical symptoms in ADHD populations. For example, increased connectivity within the auditory/sensorimotor network has been associated with more severe hyperactive/impulsive symptoms.[17] Persistent inattention symptoms in ADHD have been linked to disrupted connectivity within the default mode network (DMN) and between the DMN and task-positive networks, including the frontoparietal network (FPN) and dorsal/ventral attention networks (DAN/VAN),[18] supporting the DMN interference hypothesis.[19] Aberrant RSFC has also been associated with cognitive deficits and co-occurring conditions. For instance, altered connectivity of the frontoparietal control network (FPN) relates to impulsivity, oppositional-defiant behaviors, and impaired response inhibition and attentional control.[20] Furthermore, disrupted Salience Network (SAN)-DMN connectivity may contribute to executive function deficits in adults with ADHD, particularly working memory impairments.[21] Together, these findings suggest that ADHD-related RSFC alterations are not confined to a single network, but involve both higher-order association networks, such as the FPN, VAN, SAN, and DMN, and lower-order sensory/sensorimotor networks. More recent evidence further indicates that ADHD may be characterized by an imbalanced interplay between higher-order cognitive networks and lower-order sensory networks, such as hypoconnectivity between the SAN and auditory/sensorimotor networks.[16] Collectively, these findings suggest that RSFC captures critical information underlying the neurobiological mechanisms of ADHD.

However, most previous RSFC studies have primarily focused on case-control group differences or associations with single behavioral domains, such as inattention, hyperactivity/impulsivity, or executive function. Such approaches provide limited insight into the substantial interindividual heterogeneity within the ADHD population, where multiple clinical symptoms, cognitive abilities, and co-occurring behavioral problems often vary simultaneously. To better characterize interindividual variability and facilitate

translational applications in clinical practice, it is necessary to examine multivariate associations between RSFC patterns and multidimensional behavioral profiles in individuals with ADHD.

To better capture interindividual variability in ADHD, we examined the relationships between RSFC and a comprehensive set of ADHD-related measures, including symptoms, neurocognitive impairments, and co-occurring mental health and functional difficulties, by applying PLSC to uncover the multivariate brain-behavior associations in children with ADHD. Building on this approach, we formulated three key research questions to guide our investigation, moving from identifying multivariate brain-behavior associations using PLSC, to examining their neurobiological relevance at the neuromolecular level, and finally to assessing their predictive performance in independent datasets. Specifically, we addressed the following three research questions: (1) What latent covariance patterns can be identified between multidomain ADHD-related behaviors and RSFC? (2) Do the identified RSFC pattern(s) show spatial correspondence with the distributions of ADHD-related neurotransmitter systems, and if so, which systems are implicated? (3) To what extent can the identified RSFC pattern(s) predict ADHD symptoms in independent datasets?

Methods

Participants and clinical assessments

Discovery dataset

A total of 117 children (aged 6-12 years) with ADHD were recruited from the Children's Hospital of Chongqing Medical University. The study was approved by the Medical Ethics Committee of the Children's Hospital of Chongqing Medical University (Ethics approval number: 527-2022). Written informed consent was obtained from all parents or guardians. All participants were diagnosed with ADHD by developmental, behavioral, and/or psychiatric specialists based on the DSM-5 criteria. To exclude other developmental disorders (e.g., autism spectrum disorder) and psychotic disorders (e.g., schizophrenia), specialists conducted comprehensive clinical interviews with the children with ADHD using the Child Psychiatric Disorders Screening Questionnaire and the Kiddie-SADS–Present and Lifetime Version (K-SADS-PL). Inclusion criteria were as follows: (1) age between 6 and 12 years; (2) full-scale IQ ≥ 80 on the Wechsler Intelligence Scale for Children-Fourth Edition (WISC-IV); (3) no history of psychopharmacological treatment, or washout at least 24 hours before data collection. Exclusion criteria were as follows: (1) inability to follow instructions or comprehend tasks; (2) contraindications for MRI; (3) mean framewise displacement (FD) > 0.5 mm during rs-fMRI scanning.[22] Following data acquisition and quality control (Supplementary Fig. S1), the final sample comprised 104 children with ADHD. See Table 1 for detailed demographic and clinical characteristics of all participants in the present study.

Behavioral assessments included ADHD symptoms, cognitive functions, and co-occurring mental and functional conditions, evaluated using three scales and six neuropsychological tests. The scales were completed by parents or guardians, while the neuropsychological tests were administered to children

with ADHD via computer. ADHD symptoms and co-occurring conditions were measured using the Test of Variables of Attention (TOVA),[23] the Swanson, Nolan, and Pelham Rating Scale (SNAP-IV),[24] and the Strengths and Difficulties Questionnaire (SDQ).[25] Cognitive functions were assessed with the Behavior Rating Inventory of Executive Function, Second Edition (BRIEF-2),[26] covering nine domains of executive function, the Go/No-Go task (GNG)[27] for response inhibition, the Simon task for interference inhibition,[28] the 1-back task for working memory,[29] the Iowa Gambling Task (IGT)[30] for affective decision-making, and the Balloon Analog Risk Task (BART)[31] for risk-taking propensity. The variables assessed by these scales and tasks in this study are detailed in online Supplementary Methods 1.1.1 and Table 1.

External validation dataset 1

An independent pediatric validation sample was obtained from the Healthy Brain Network (HBN) Biobank, an open-access pediatric neuroimaging resource established by the Child Mind Institute that includes clinical, behavioral, cognitive, and multimodal neuroimaging data from children and adolescents.[32] To ensure consistency with the inclusion criteria of the discovery sample, participants were included if they: (1) were aged 6–12 years; (2) had a consensus clinical diagnosis of ADHD using the DSM-5; (3) had no comorbid psychiatric or neurodevelopmental diagnoses; (4) had available ADHD core symptom data assessed using the Strengths and Weaknesses Assessment of Normal Behavior Rating Scale for ADHD (SWAN);[24] (5) had both resting-state fMRI runs available, with each run containing more than 370 volumes and a mean FD smaller than 0.5 mm; (6) had the T1-weighted structural images available. The final sample comprised 60 children with ADHD, including 25 girls (41.67%), with a mean age of 9.13 years (SD = 1.35). Further details of the SWAN and demographic characteristics are provided in Supplementary Methods 1.1.2 and Table S1.

External validation dataset 2

A total of 256 university students participated in rs-fMRI acquisition and completed the Adult ADHD Self-Report Scale (ASRS)[33]. Participants were recruited from the Behavioral Brain Research Project of Chinese Personality (BBP) at Southwest University, China, and had no history of neuropsychiatric disorders or brain injury. Ethical approval was granted by the Brain Imaging Center Institutional Review Board (ID: CNPH2019016). Twenty-five individuals were excluded due to excessive head motion, defined as a mean FD > 0.2 mm or >10% outlier volumes. The final sample comprised 231 participants (163 females, 70.56%), with a mean age of 22.01 years (SD = 0.91, range = 19–25). The ASRS provides score ranges for identifying ADHD: scores from 0 to 16 suggest minimal attention and hyperactive/impulsive deficits; scores between 17 and 23 indicate possible deficits; scores above 23 strongly suggest the presence of these deficits.[34,35] Using a cutoff of 17, we identified individuals with higher ADHD traits for external validation. The high-ADHD trait group comprised 75 individuals (mean age = 22.04, SD = 0.99, age range 20-25 years) who scored above 17 on either the ASRS-I, ASRS-HI, or both subscales. Further details are provided in Supplementary Methods 1.1.3 and Table S2.

MR data acquisition and preprocessing

Discovery dataset

All children with ADHD underwent resting-state functional MRI (rs-fMRI) and high-resolution T1-weighted MRI using a 3-T scanner (Siemens Prisma, Erlangen, Germany). To alleviate anxiety and acclimate the children to the scanning environment, the experimenters introduced them to a mock scanner simulating the scanning process. During scanning, children wore earplugs and used foam padding to minimize head movement and reduce machine noise. Each child completed an 8-minute rs-fMRI scan, acquiring functional images using a gradient echo planar imaging sequence. The scanning parameters were as follows: repetition time (TR) of 750 ms; echo time (TE) of 30 ms; field of view (FOV) of 216×216 mm^2； number of slices of 60; slice thickness of 2.4 mm; voxel size of 2.4×2.4×2.4 mm^3; matrix size of 90×90; and flip angle (FA) of 60 degrees. A total of 640 frames of resting-state neuroimaging data were collected. Additionally, high-resolution T1-weighted structural images were obtained for registration purposes, with the following parameters: TR of 2300 ms; TE of 2.07 ms; FOV of 256×224 mm^2; number of slices of 240 ; slice thickness of 0.80 mm; voxel size of 0.8×0.8×0.8 mm^3; resolution matrix of 320×280; FA of 7 degrees. During the scan, children were instructed to keep their eyes open, stay awake, remain still, and fixate on the displayed crosshair.

MRI data were preprocessed using SPM12 and the DPARSFA (Advanced Edition) toolbox (v8.1) in MATLAB 2019a. Following the standard pipeline, individual T1-weighted images were co-registered to the mean functional images and segmented into gray matter, white matter, and cerebrospinal fluid using the DARTEL algorithm, then normalized to Montreal Neurologic Institute (MNI) space using DARTEL-derived flow fields with a resampled voxel size of 3×3×3 mm^3. Nuisance covariates were regressed out using the Friston 24-parameter model and the mean signals from white matter and CSF. Temporal band-pass filtering (0.01–0.08 Hz) and spatial smoothing with a 6 mm FWHM Gaussian kernel were applied. Due to the short TR of 750 ms, slice-timing correction and discarding the first 10 time points were omitted, as signal stabilization and temporal alignment were not substantially affected.

External validation dataset 1

Resting-state fMRI (rs-fMRI) and high-resolution T1-weighted structural images for the HBN cohort were acquired on 3-T Siemens PrismaFIT and TimTrio scanners, with identical acquisition protocols across scanners. Functional images were obtained using a repetition time (TR) of 800 ms, an echo time (TE) of 30 ms, and 2.4-mm isotropic voxels. Data were preprocessed following the same pipeline as described for the discovery dataset. Detailed acquisition parameters and preprocessing procedures are provided in Supplementary Methods 1.2.1 and on the HBN website (https://fcon_1000.projects.nitrc.org/indi/cmi_healthy_brain_network/).

External validation dataset 2

The rs-fMRI and high-resolution T1-weighted images from the BBP sample were acquired using a 3-T scanner (Siemens Prisma, Erlangen, Germany) at Southwest University's Faculty of Psychology. During the resting-state scan, participants were instructed to keep their eyes closed, remain still and awake, and

avoid directed thinking. Functional images were acquired with a repetition time of 2000 ms, an echo time of 30 ms, and 2-mm isotropic voxels. Data were preprocessed using SPM12 and CONN, including removal of the first 10 volumes, slice-timing correction, realignment, normalization to Montreal Neurological Institute space, spatial smoothing, nuisance regression, motion censoring, linear detrending, and temporal filtering. Volumes with framewise displacement > 0.5 mm, together with one preceding and two subsequent volumes, were censored. Full acquisition and preprocessing details are provided in Supplementary Methods 1.2.2.

Resting-state functional connectivity (RSFC) construction

The RSFC functional network was built using the preprocessed rs-fMRI data. Brain regions were parcellated according to the Brainnetome Atlas,[36] which includes 210 cortical and 36 subcortical regions. RSFC was calculated using the rsHRF toolbox (https://www.nitrc.org/projects/rshrf) based on SPM12. The "rsHRF conn" function generated a 246×246 symmetric connectivity matrix with 30,135 [(245×246)/2] edges for each participant. Each edge represents the Pearson correlation coefficient between the time series of paired nodes. Fisher's r-to-z transformation was applied to normalize the correlation coefficients. The 210 cortical regions were assigned to one of seven large-scale resting-state networks: visual (VN), somatomotor (SMN), dorsal attention (DAN), ventral attention (VAN), limbic (LN), frontoparietal (FPN), and default mode networks (DMN). The 36 subcortical regions were grouped into a newly defined subcortical network (SBN), as they are not part of the Yeo 7 networks.[37]

Partial least squares correlation analysis (PLSC)

PLSC models the multivariate nature of both brain and behavioral data, allowing for the identification of joint brain-behavior relationships.[9] In this study, PLSC was utilized to investigate the association between RSFC and ADHD behavioral measures (Figure 1A). The analysis followed seven steps, which are detailed in the online Supplementary Methods 1.3. (1) To minimize the influence of potential confounders on PLSC results, we regressed age, sex, mean FD, IQ, and medication status from the brain and behavioral data. (2) Next, we applied singular value decomposition to the brain-behavior covariance matrix to identify latent brain-behavior dimensions/components. Each latent component (LC) consists of an RSFC pattern at the node level (referred to as RSFC saliences) and a corresponding behavioral profile (termed behavioral saliences). (3) A permutation test with 5000 iterations was conducted to identify significant LCs, and the permutation p-values for the top five LCs were adjusted for multiple comparisons using a false discovery rate (FDR) of $q < .05$. (4) Behavioral and RSFC composite scores were computed by linearly projecting each child's RSFC and behavioral data onto the corresponding saliences. The primary objective of PLSC is to identify saliences that maximize the covariance between RSFC and behavioral composite scores across participants. (5) Behavioral loadings were computed using Pearson's correlations between the original behavioral data and the behavioral composite scores to interpret the latent components (LCs). Higher absolute values of loadings indicate greater importance of the behavioral measures for the LC. The RSFC loadings were calculated similarly. (6) A bootstrapping procedure was applied, generating 1000 samples from the RSFC and behavioral data to estimate

confidence intervals for the loadings. Z-scores were calculated by dividing each correlation coefficient by its bootstrapped standard deviation. To reduce multiple comparisons, bootstrapped correlations between RSFC data and composite scores were averaged across region pairs within and between eight networks, resulting in 8 × 8 correlation matrices prior to Z-score computation. These Z-scores were converted to p-values and adjusted using the false discovery rate (FDR) ($q < .05$). (7) To ensure the robustness of the LCs, we performed 5-fold cross-validation of the PLSC analysis.

Spatial correlation with neurotransmitter densities

To examine the spatial metabolic substrates of RSFC patterns associated with ADHD identified by PLSC analysis, we conducted spatial correlation analyses between RSFC loadings and the densities of several neurotransmitter systems implicated in ADHD (Figure 1B). Prior evidence indicates that dopamine receptors (D1, D2), dopamine transporter (DAT), noradrenaline transporters (NET), serotonin transporters (5-HTT), and histamine receptors (H3) play critical roles in the onset and clinical progression of ADHD.[38-41] Based on a molecular imaging study,[42] we obtained group average spatial distribution maps for six neurotransmitters from 104 healthy volunteers (D1: n = 13; D2: n = 37; DAT: n = 6; NET: n = 10; 5HTT: n = 30; H3: n = 8). These maps were resampled to an isotropic 3 mm resolution, consistent with the rs-fMRI data. Using the Brainnetome Atlas applied in rs-fMRI preprocessing, we calculated the average values for 246 regions, resulting in a 246×6 matrix. The absolute RSFC loading values were then summed for each Brainnetome Atlas region to derive region importance scores (246×1). Finally, Spearman correlation analyses were performed between the regional importance scores and the spatial distribution of each receptor or transporter. Statistical significance was assessed using spatial permutation tests that accounted for the spatial autocorrelation of brain regions.[43] A null distribution of correlation coefficients was generated from 5,000 permutations between regional importance scores and neurotransmitter densities. Empirical p-values were derived by comparing the observed spatial correlations with the null distribution, with significance defined at FDR-corrected $p < 0.05$.

External prediction validation

We further evaluated whether the RSFC spatial pattern of the significant LC could predict ADHD symptoms in unrelated individuals from the HBN and BBP datasets (Figure 1C). Elastic-net regression with 5-fold cross-validation was employed to mitigate multicollinearity during feature selection.[44,45] Hyperparameters—alpha (10^{-7} to 1) and thresholds (0.05, 0.01, 0.005, 0.001, 0.0005, 0.0001)—were tested in pairs. To enhance stability, each pair underwent 100 repetitions of 5-fold cross-validation, and the resulting predicted scores were averaged to obtain robust estimates. Detailed procedures are provided in Supplementary Methods 1.4. Predictive performance was quantified as the Spearman correlation p-value between predicted and observed scores. Additionally, significance was assessed via 2000 permutation tests, in which brain-behavior pairings were randomized and the 5-fold cross-validation repeated.

Results

PLSC model reveals one robust latent component (LC) linking ADHD Behavioral Domains and resting-state function connectivity (RSFC)

Figure 2A shows the amount of covariance explained by each LC. Only LC (LC1) that survived after permutation testing with FDR correlation ($q < 0.05$). The LC1 accounted for 24.70% of the covariance between RSFC and behavioral measures. The behavioral composite scores and the RSFC composite scores were significantly correlated (r = 0.72; Figure 2B). The 5-fold cross-validation was successful (test folds, mean r = 0.21, permuted p < .001). Following 1000 bootstrap iterations, 24 of the 35 ADHD behavioral measures demonstrated significant loadings (Figure 2C). These encompassed nearly all clinical symptoms, cognitive functions, and co-occurring conditions of ADHD.

Correlations between LC1's RSFC composite scores and RSFC among 210 cortical and 36 subcortical ROIs are presented in Figure 2D (unthresholded) and Figure 2E (significant correlations). Figure 2F depicts the significant RSFC correlations averaged within and between the seven networks defined by Yeo et al. Higher RSFC composite scores were associated with increased connectivity between the VAN and SBN, SMN and SBN, VAN and DMN, and SMN and DMN, and with decreased connectivity between the SMN and VN, and VAN and VN. To illustrate the relative contribution of individual regions to this significant RSFC pattern, the top ten nodes with the highest weighted degree are reported in Supplementary Table S3. These nodes were predominantly located within the VAN and SMN. Collectively, these findings suggest that disrupted connectivity between the VAN and other networks, as well as between the SMN and other networks, plays a pivotal role in the clinical symptoms, neurocognitive deficits, and co-occurring conditions observed in children with ADHD.

Spatial correlation with neurotransmitter densities

We examined whether the ADHD-related connectome was spatially associated with neurotransmitter systems implicated in ADHD, including dopamine receptors (D1, D2, DAT), noradrenaline transporters (NET), serotonin transporters (5-HTT), and histamine receptors (H3). Figure 3A summarizes RSFC loadings for each Brainconnectome atlas region, representing regional importance scores. Permutation testing with FDR correction ($q < 0.05$) revealed significant correlations between regional importance scores and the spatial distribution of D1, D2, DAT, H3, NET, and 5-HTT (Figure 3B). These findings indicate that the PLS pattern derived from RSFC may reflect neuromolecular mechanisms relevant to ADHD.

Predictive utility of the ADHD-related connectome for clinical symptoms in External validation Datasets

We assessed the predictive utility of ADHD-related connectome features for individual ADHD symptoms scores across two independent datasets using elastic-net regression. The HBN dataset included children diagnosed with ADHD, while the BBP dataset consisted of high-trait ADHD emerging adults. Results showed that the significant edges of the ADHD-related connectome identified in the discovery sample predicted symptom scores (total SWAN scores) in the HBN dataset. The predicted and actual scores were significantly correlated (r = 0.373, p = 0.003, permuted p = 0.003) after 100 repeats of 5-fold cross-

validation (alpha = 0.2, threshold = 0.05; Figure 4A). We also compared models based on the ADHD-related connectome to those using the whole-brain connectome. The ADHD-related connectome models showed better prediction performance ($r = 0.261$, $p = 0.044$, permuted $p = 0.016$; alpha = 0.2, threshold = 0.05; Figure 4B). Similarly, significant edges identified by the PLSC analysis predicted ADHD symptoms (total ASRS scores) in the BBP dataset ($r = 0.445$, $p < 0.001$, permuted $p = 0.001$; alpha = 0.1, threshold = 0.01; Figure 4C), with better performance than whole-brain models ($r = 0.330$, $p = 0.005$, permuted $p < 0.001$; Figure 4D). These findings demonstrate that the ADHD-related connectome enables individual-level prediction of ADHD symptoms across different populations.

Discussion

ADHD is a heterogeneous disorder, characterized by substantial individual variability in symptom profiles, neurocognitive impairments, co-occurring problems, and patterns of brain dysfunction. Capturing this heterogeneity requires moving beyond categorical comparisons toward dimensional approaches that can characterize multivariate brain-behavior associations. In the present study, we identified a significant latent pattern linking RSFC to multidomain ADHD-related measures in children with ADHD. This pattern showed a strong brain-behavior association ($r = 0.72$) and accounted for 24.7% of the explained covariance. At the behavioral level, this dimension was characterized by contributions from 24 of the 35 ADHD-related measures, spanning clinical symptoms, neurocognitive functions, and co-occurring problems. At the neural level, the corresponding RSFC pattern was primarily characterized by altered connectivity involving the VAN and SMN. Importantly, regional importance scores derived from the RSFC pattern were significantly associated with the spatial distributions of several neurotransmitters implicated in ADHD, including D1, D2, DAT, H3, NET, and 5-HTT. Moreover, the RSFC pattern significantly predicted ADHD symptoms in both HBN and BBP datasets. The results of neurotransmitters and predicting supports the robustness and generalizability of the PLSC findings. Collectively, these findings identify a biologically meaningful RSFC pattern related to multidomain ADHD variability, highlighting its potential for developing connectome-based biomarkers relevant to ADHD treatment.

Kebets et al. identified three transdiagnostic dimensions involving somatomotor dysconnectivity, suggesting that sensory–motor circuitry may broadly contribute to psychiatric symptoms and cognitive–behavioral dysfunction.[46] More recently, Gallucci et al. showed that bilateral DLPFC rTMS selectively reduced a PLSC-derived general depressive symptom dimension involving DLPFC-centered FPN, DMN, and CON circuits, but not other dimensions.[47] Together, these findings indicate that latent connectivity–behavior dimensions may inform circuit-based interventions. Accordingly, the SMN- and VAN-related RSFC pattern identified here warrants further investigation as a candidate circuit signature for symptom stratification and treatment-response monitoring in ADHD.

The dimension identified in the present study may reflect an integrated profile spanning symptoms, cognitive functions, and co-occurring difficulties, rather than a dimension defined by core symptoms alone.[48] Notably, inattention, inhibition, and ODD emerged as the strongest contributors within the clinical symptom, cognitive function, and co-occurring condition domains, respectively. Inattention is a

particularly important symptom dimension in school-aged children with ADHD, as it is closely associated with subsequent functional impairments, including poorer academic and educational outcomes and socioeconomic disadvantage in adulthood.[49–51] Meanwhile, inhibitory control is regarded as a key endophenotype of ADHD, with individuals showing better inhibition tending to have a more stable or improved trajectory of inattentive symptoms.[52] Longitudinal evidence further suggests that early ADHD symptoms may increase the risk of later argumentative and defiant behaviors, supporting a developmental link between ADHD-related difficulties and ODD symptoms.[53] One possible interpretation is that impaired inhibitory control may hinder the suppression of irrelevant stimuli, task-unrelated thoughts, and inappropriate responses, thereby contributing to inattention. In turn, persistent inattentive difficulties may increase negative interactions in daily contexts, potentially fostering ODD-related behaviors. Although this pathway remains to be tested in longitudinal and mechanistic studies, these findings underscore the importance of considering ADHD as an interaction among clinical symptoms, neurocognitive processes, and co-occurring conditions.

The RSFC pattern of the latent dimension consisted of the 10 highest-degree nodes in the VAN and SMN, suggesting that these networks may function as key hubs in ADHD. VAN mainly includes the temporoparietal junction, inferior frontal gyrus, and anterior insula, and functions as a task-positive network responsible for detecting salient stimuli and regulating the switch between externally oriented attention and internally directed mentation.[54] When VAN fails to appropriately reorient attention to task-relevant stimuli, the DMN may become inappropriately engaged, resulting in lapses of attention.[19] Consistent with previous findings, abnormal functional connectivity between VAN and DMN has been observed in both children and adults with ADHD, reflecting impaired suppression of internally directed thoughts during task performance, which contributes to mind-wandering and attentional fluctuations.[55] Beyond VAN-DMN interactions, the present study also identified disrupted connectivity between VAN and SBN, which are critical for executive control and behavioral regulation. Impaired VAN-SBN connectivity may prevent salient signals detected by VAN from effectively reaching the SBN, compromising bottom-up regulation of attention and behavior, and thereby contributing to core ADHD symptoms such as inattention and impulsivity/hyperactivity. Together, these findings support the notion that functional abnormalities in both cortical attention networks and fronto-subcortical circuits constitute a neurobiological basis for ADHD.[56–59]

The SMN, primarily comprising the precentral gyrus, postcentral gyrus, and supplementary motor area, is responsible for somatosensory processing and motor coordination.[60] Previous studies have shown that functional connectivity within the SMN increases with age in children with ADHD—opposite to the typical developmental trajectory—and that this atypical pattern is associated with symptom severity.[61] This may reflect an impaired ability to decode sensory information, whereby deficits at lower-level sensory processing cascade upward and disrupt higher-order cognitive functions,[62] consistent with the developmental framework proposed by Zelazo (2020),[63] which posits that atypical maturation of lower-order networks can interfere with the later development of prefrontal executive systems. In the present study, aberrant functional connectivity between the SMN and both the DMN and SBN was associated

with ADHD. Recent evidence further indicates that altered SMN–DMN connectivity correlates with the severity of hyperactivity/impulsivity symptoms in children with ADHD.[64] This suggests that abnormal DMN influence on SMN activity may increase susceptibility to internally generated, task-irrelevant interference during action preparation and inhibition, thereby contributing to core behavioral symptoms.[65] Similarly, prior work has linked disrupted connectivity between the primary motor cortex and basal ganglia to ADHD symptomatology,[66] supporting the notion that SMN–SBN dysconnectivity may underlie deficits in sensorimotor integration. Such impairments may hinder the efficient transformation of sensory input into appropriate motor responses, ultimately affecting motor coordination, attention, and impulse control. Taken together, our findings suggest that abnormal functional connectivity involving the VAN and SMN, particularly their interactions with the DMN and SBN, may constitute a basis of ADHD, providing a clear direction for future neuroregulation interventions and the quantification of intervention effects.

The RSFC pattern derived from the identified dimension showed significant spatial correlations with multiple neurotransmitter systems implicated in ADHD, including dopamine receptors (D1, D2), dopamine transporter (DAT), noradrenaline transporter (NET), serotonin transporter (5-HTT), and histamine receptor (H3). These findings suggest that the RSFC-derived pattern is neurobiologically meaningful and reflects underlying neuromolecular mechanisms associated with ADHD. Furthermore, elastic-net regression models demonstrated that the significant edges of the ADHD-related connectome identified in the discovery sample reliably predicted inattention scores in two independent datasets (HBN and BBP). These results indicate that the identified connectome is robust and effectively captures interindividual variability within the ADHD population.

In summary, we identified multivariate patterns of intrinsic functional connectivity that are strongly associated with a specific ADHD-related dimension in children. This dimension integrates a distinct cluster of behavioral measures with characteristic RSFC features. The identified RSFC pattern showed spatial correspondence with the distribution of several neurotransmitter systems implicated in ADHD and reliably predicted inattentive symptoms across two independent datasets. Together, these findings delineate a connectivity-guided dimension of ADHD that captures meaningful neurobiological and behavioral variability. This framework advances our understanding of the neurobiology underlying ADHD and provides a promising foundation for the development of connectome-based biomarkers, with potential implications for more precise diagnosis and targeted interventions.

This study has several limitations. First, while we focused on RSFC and behavioral measures of ADHD, future research should incorporate multimodal imaging data and objective ADHD assessments, including physiological indicators such as heart rate variability, body movement, and eye tracking. Second, the discovery sample primarily comprised children aged 6–12 years, highlighting the need for future studies to examine RSFC-informed ADHD dimensions across a broader age range, including both younger and older populations. Third, the correlational nature of the present findings does not allow us to determine causal relationships between the identified RSFC pattern and ADHD-related behavioral characteristics. Longitudinal studies with repeated neuroimaging and behavioral assessments are

needed to examine their temporal and potentially bidirectional relationships. More importantly, experimental intervention studies that directly target relevant neural circuits or ADHD-related behaviors are needed to determine whether changes in the identified RSFC pattern lead to improvements in ADHD-related symptoms and functioning, or whether improvements in ADHD-related behavioral characteristics lead to changes in the identified RSFC pattern.

Declarations

Competing interests

The authors declare that they have no conflict of interest.

Acknowledgements

This study was supported by Science and Brain-like Intelligence Technology-National Science and Technology Major Project(2026ZD0222603), the National Natural Science Foundation of China (32271123, 32571253) and the Fundamental Research Funds for the Central Universities (SWU2609105).

References

1. Popit S, Serod K, Locatelli I, Stuhec M. Prevalence of attention-deficit hyperactivity disorder (ADHD): systematic review and meta-analysis. Eur Psychiatry 2024; 67: e68.
2. Polanczyk G, de Lima MS, Horta BL, Biederman J, Rohde LA. The worldwide prevalence of ADHD: a systematic review and metaregression analysis. Am J Psychiatry 2007; 164: 942–948.
3. Polanczyk GV, Willcutt EG, Salum GA, Kieling C, Rohde LA. ADHD prevalence estimates across three decades: an updated systematic review and meta-regression analysis. Int J Epidemiol 2014; 43: 434–442.
4. Willcutt EG. The prevalence of DSM-IV attention-deficit/hyperactivity disorder: a meta-analytic review. Neurotherapeutics 2012; 9(3): 490–499.
5. Faraone SV, Banaschewski T, Coghill D, Zheng Y, Biederman J, Bellgrove MA et al. The World Federation of ADHD International Consensus Statement: 208 Evidence-based conclusions about the disorder. Neurosci Biobehav Rev 2021; 128: 789–818.
6. Faraone SV, Bellgrove MA, Brikell I, Cortes S, Hartman CA, Hollis C et al. Attention-deficit/hyperactivity disorder. Nat Rev Dis Primers 2024; 10: 11.
7. Luo L, Chen L, Wang Y, Li Q, He N, Li Y et al. Patterns of brain dynamic functional connectivity are linked with attention-deficit/hyperactivity disorder-related behavioral and cognitive dimensions. Psychol Med 2023; 53: 6666–6677.

8. Wang Y, Genon S, Dong D, Zhou F, Li C, Yu D et al. Covariance patterns between sleep health domains and distributed intrinsic functional connectivity. Nat Commun 2023; 14: 7133.
9. Vieira S, Bolton TAW, Schöttner M, Baecker L, Marquand A, Mechelli A et al. Multivariate brain-behaviour associations in psychiatric disorders. Transl Psychiatry 2024; 14: 231.
10. Mei T, Llera A, Floris DL, Forde NJ, Tillmann J, Durston S et al. Gray matter covariations and core symptoms of autism: the EU-AIMS Longitudinal European Autism Project. Mol Autism 2020; 11: 86.
11. Li Q, Zhao Y, Hu Y, Liu Y, Wang Y, Zhang Q et al. Linked patterns of symptoms and cognitive covariation with functional brain controllability in major depressive disorder. EBioMedicine 2024; 106: 105255.
12. Lin HY, Cocchi L, Zalesky A, Lv J, Perry A, Tseng WI et al. Brain-behavior patterns define a dimensional biotype in medication-naïve adults with attention-deficit hyperactivity disorder. Psychol Med 2018; 48: 2399–2408.
13. Kilpatrick LA, Joshi SH, O'Neill J, Kalender G, Dillon A, Best KM et al. Cortical gyrification in children with attention deficit-hyperactivity disorder and prenatal alcohol exposure. Drug Alcohol Depend 2021; 225: 108817.
14. Tsai CJ, Lin HY, Tseng IW, Gau SS. White matter microstructural integrity correlates of emotion dysregulation in children with ADHD: A diffusion imaging tractography study. Prog Neuropsychopharmacol Biol Psychiatry 2021; 110: 110325.
15. Gao Y, Shuai D, Bu X, Hu X, Tang S, Zhang L et al. Impairments of large-scale functional networks in attention-deficit/hyperactivity disorder: a meta-analysis of resting-state functional connectivity. Psychol Med 2019; 49: 2475–2485.
16. Gao Y, Zhou Z, Bao W, Chen Y, Hu X, Li H et al. Multiscale functional connectivity reveals imbalanced interplay between higher-and lower-order brain networks in ADHD. Nat Mental Health 2025; 3: 1331–1341.
17. Sörös P, Hoxhaj E, Borel P, Sadohara C, Feige B, Matthies S et al. Hyperactivity/restlessness is associated with increased functional connectivity in adults with ADHD: a dimensional analysis of resting state fMRI. BMC Psychiatry 2019; 19: 43.
18. Sudre G, Szekely E, Sharp W, Kasparek S, Shaw P. Multimodal mapping of the brain's functional connectivity and the adult outcome of attention deficit hyperactivity disorder. Proc Natl Acad Sci U S A 2017; 114: 11787–11792.
19. Sonuga-Barke EJ, Castellanos FX. Spontaneous attentional fluctuations in impaired states and pathological conditions: a neurobiological hypothesis. Neurosci Biobehav Rev 2007; 31: 977–986.
20. Lin HY, Tseng WY, Lai MC, Matsuo K, Gau SS. Altered resting-state frontoparietal control network in children with attention-deficit/hyperactivity disorder. J Int Neuropsychol Soc 2015; 21: 271–284.
21. Zhao Q, Li H, Yu X, Huang F, Wang Y, Liu L et al. Abnormal Resting-State Functional Connectivity of Insular Subregions and Disrupted Correlation with Working Memory in Adults with Attention Deficit/Hyperactivity Disorder. Front Psychiatry 2017; 8: 200.

22. Cai W, Warren SL, Duberg K, Pennington B, Hinshaw SP, Menon V. Latent brain state dynamics distinguish behavioral variability, impaired decision-making, and inattention. Mol Psychiatry 2021; 26: 4944–4957.
23. Pollock B, Harrison AG, Armstrong IT. What can we learn about performance validity from TOVA response profiles? J Clin Exp Neuropsychol 2021; 43: 412–425.
24. Swanson JM, Schuck S, Porter MM, Carlson C, Hartman CA, Sergeant JA et al. Categorical and Dimensional Definitions and Evaluations of Symptoms of ADHD: History of the SNAP and the SWAN Rating Scales. Int J Educ Psychol Assess 2012; 10: 51–70.
25. Goodman R, Meltzer H, Bailey V. The Strengths and Difficulties Questionnaire: a pilot study on the validity of the self-report version. Int Rev Psychiatry 2003; 15: 173–177.
26. Gioia GA, Isquith PK, Kenworthy L, Barton RM. Profiles of everyday executive function in acquired and developmental disorders. Child Neuropsychol 2002; 8: 121–137.
27. Wodka EL, Mahone EM, Blankner JG, Larson JC, Fotedar S, Denckla MB et al. Evidence that response inhibition is a primary deficit in ADHD. J Clin Exp Neuropsychol 2007; 29: 345–356.
28. Davidson MC, Amso D, Anderson LC, Diamond A. Development of cognitive control and executive functions from 4 to 13 years: evidence from manipulations of memory, inhibition, and task switching. Neuropsychologia 2006; 44: 2037–2078.
29. Vuontela V, Steenari MR, Carlson S, Koivisto J, Fjällberg M, Aronen ET. Audiospatial and visuospatial working memory in 6–13 year old school children. Learn Mem 2003; 10: 74–81.
30. Bechara A, Damasio AR, Damasio H, Anderson SW. Insensitivity to future consequences following damage to human prefrontal cortex. Cognition 1994; 50: 7–15.
31. Lejuez CW, Read JP, Kahler CW, Richards JB, Ramsey SE, Stuart GL et al. Evaluation of a behavioral measure of risk taking: the Balloon Analogue Risk Task (BART). J Exp Psychol Appl 2002; 8: 75–84.
32. Alexander LM, Escalera J, Ai L, Febre K, Mangone A, Vega-Potler N et al. An open resource for transdiagnostic research in pediatric mental health and learning disorders. Sci Data 2017; 4: 170181.
33. Kessler RC, Adler L, Ames M, Demler O, Faraone S, Hiripi E et al. The World Health Organization Adult ADHD Self-Report Scale (ASRS): a short screening scale for use in the general population. Psychol Med 2005; 35: 245–256.
34. Wernicke J, Li M, Sha P, Zhou M, Sindermann C, Becker B et al. Individual differences in tendencies to attention-deficit/hyperactivity disorder and emotionality: empirical evidence in young healthy adults from Germany and China. Atten Defic Hyperact Disord 2019; 11: 167–182.
35. Yeh CB, Gau SS, Kessler RC, Wu YY. Psychometric properties of the Chinese version of the adult ADHD Self-report Scale. Int J Methods Psychiatr Res 2008; 17: 45–54.
36. Fan L, Li H, Zhuo J, Zhang Y, Wang J, Chen L et al. The Human Brainnetome Atlas: A New Brain Atlas Based on Connectional Architecture. Cereb Cortex 2016; 26: 3508–3526.

37. Yeo BT, Krienen FM, Sepulcre J, Sabuncu MR, Lashkari D, Hollinshead M et al. The organization of the human cerebral cortex estimated by intrinsic functional connectivity. J Neurophysiol 2011; 106: 1125–1165.
38. Faraone SV. The pharmacology of amphetamine and methylphenidate: Relevance to the neurobiology of attention-deficit/hyperactivity disorder and other psychiatric comorbidities. Neurosci Biobehav Rev 2018; 87: 255–270.
39. Radonjić NV, Bellato A, Khoury NM, Cortese S, Faraone SV. Nonstimulant Medications for Attention-Deficit/Hyperactivity Disorder (ADHD) in Adults: Systematic Review and Meta-analysis. CNS Drugs 2023; 37: 381–397.
40. Vohora D, Bhowmik M. Histamine H3 receptor antagonists/inverse agonists on cognitive and motor processes: relevance to Alzheimer's disease, ADHD, schizophrenia, and drug abuse. Front Syst Neurosci 2012; 6: 72.
41. Faraone SV, Ward CL, Boucher M, Elbekai R, Brunner E. Role of serotonin in psychiatric and somatic comorbidities of attention-deficit/hyperactivity disorder: a systematic literature review. Neurosci Biobehav Rev 2025; 176: 106275.
42. Hansen JY, Shafiei G, Markello RD, Smart K, Cox SML, Nørgaard M et al. Mapping neurotransmitter systems to the structural and functional organization of the human neocortex. Nat Neurosci 2022; 25: 1569–1581.
43. Burt JB, Helmer M, Shinn M, Anticevic A, Murray JD. Generative modeling of brain maps with spatial autocorrelation. Neuroimage 2020; 220: 117038.
44. Xiao Z, Chen Z, Chen W, Gao W, He L, Wang Q et al. Maladaptive changes in delay discounting in males during the COVID-19 pandemic: the predictive role of functional connectome. Cereb Cortex 2022; 32: 4605–4618.
45. Yin Y, Su T, Wang X, Hu B, Zhang R, Zhou F et al. Exploring common and distinct neural basis of procrastination and impulsivity through elastic net regression. Cereb Cortex 2025; 35: bhae503.
46. Kebets V, Holmes AJ, Orban C, Tang S, Li J, Sun N et al. Somatosensory-Motor Dysconnectivity Spans Multiple Transdiagnostic Dimensions of Psychopathology. Biol Psychiatry 2019; 86: 779–791.
47. Gallucci J, Yu JC, Oliver LD, Nakua H, Zhukovsky P, Dickie EW et al. Neural Circuitry and Therapeutic Targeting of Depressive Symptoms in Schizophrenia Spectrum Disorders. Am J Psychiatry 2024; 181: 910–919.
48. Yang Y, Shields GS, Zhang Y, Wu H, Chen H, Romer AL. Child executive function and future externalizing and internalizing problems: A meta-analysis of prospective longitudinal studies. Clin Psychol Rev 2022; 97: 102194.
49. Pingault JB, Tremblay RE, Vitaro F, Carbonneau R, Genolini C, Falissard B et al. Childhood trajectories of inattention and hyperactivity and prediction of educational attainment in early adulthood: a 16-year longitudinal population-based study. Am J Psychiatry 2011; 168: 1164–1170.

50. Merrell C, Sayal K, Tymms P, Kasim A. A longitudinal study of the association between inattention, hyperactivity and impulsivity and children's academic attainment at age 11. Learn Individ Differ 2017; 53: 156–161.
51. Galéra C, Bouvard MP, Lagarde E, Michel G, Touchette E, Fombonne E et al. Childhood attention problems and socioeconomic status in adulthood: 18-year follow-up. Br J Psychiatry 2012; 201: 20–25.
52. Pang T, Yang L, Liu Y, Chang S. The trajectory of attention deficit hyperactivity disorder symptoms and its dynamic relationship with inhibitory control. J Child Psychol Psychiatry 2025; 66: 980–993.
53. Harvey EA, Breaux RP, Lugo-Candelas CI. Early development of comorbidity between symptoms of attention-deficit/hyperactivity disorder (ADHD) and oppositional defiant disorder (ODD). J Abnorm Psychol 2016; 125: 154–167.
54. Menon V. Large-scale brain networks and psychopathology: a unifying triple network model. Trends Cogn Sci 2011; 15: 483–506.
55. Guo X, Yao D, Cao Q, Liu L, Zhang Q, Li H et al. Shared and distinct resting functional connectivity in children and adults with attention-deficit/hyperactivity disorder. Transl Psychiatry 2020; 10: 65.
56. Rubia K, Alegria A, Brinson H. Imaging the ADHD brain: disorder-specificity, medication effects and clinical translation. Expert Rev Neurother 2014; 14: 519–538.
57. Zhu Y, Jiang X, Ji W. The Mechanism of Cortico-Striato-Thalamo-Cortical Neurocircuitry in Response Inhibition and Emotional Responding in Attention Deficit Hyperactivity Disorder with Comorbid Disruptive Behavior Disorder. Neurosci Bull 2018; 34: 566–572.
58. Posner J, Park C, Wang Z. Connecting the dots: a review of resting connectivity MRI studies in attention-deficit/hyperactivity disorder. Neuropsychol Rev 2014; 24: 3–15.
59. Xia S, Li X, Kimball AE, Kelly MS, Lesser I, Branch C. Thalamic shape and connectivity abnormalities in children with attention-deficit/hyperactivity disorder. Psychiatry Res 2012; 204: 161–167.
60. Uddin LQ, Yeo BTT, Spreng RN. Towards a Universal Taxonomy of Macro-scale Functional Human Brain Networks. Brain Topogr 2019; 32: 926–942.
61. Marcos-Vidal L, Martínez-García M, Pretus C, Garcia-Garcia D, Martínez K, Janssen J et al. Local functional connectivity suggests functional immaturity in children with attention-deficit/hyperactivity disorder. Hum Brain Mapp 2018; 39: 2442–2454.
62. Javitt DC, Freedman R. Sensory processing dysfunction in the personal experience and neuronal machinery of schizophrenia. Am J Psychiatry 2015; 172: 17–31.
63. Zelazo PD. Executive Function and Psychopathology: A Neurodevelopmental Perspective. Annu Rev Clin Psychol 2020; 16: 431–454.
64. Chen S, Lu C, Xue B, Zhou R, Bai X, Cheng Y et al. Intrinsic functional connectivity alterations in medication-naïve children with combined and inattentive ADHD types: Evidence from cortical surface-based analysis. J Affect Disord 2026; 406: 121718.

65. Duffy KA, Rosch KS, Nebel MB, Seymour KE, Lindquist MA, Pekar JJ et al. Increased integration between default mode and task-relevant networks in children with ADHD is associated with impaired response control. Dev Cogn Neurosci 2021; 50: 100980.
66. McLeod KR, Langevin LM, Dewey D, Goodyear BG. Atypical within- and between-hemisphere motor network functional connections in children with developmental coordination disorder and attention-deficit/hyperactivity disorder. Neuroimage Clin 2016; 12: 157–164.

Tables

Table 1. Demographic and clinical characteristics of all children with ADHD in the discovery dataset.

	Abbreviation	Mean ± S.D.	Range
Age (years)	/	9.04 ± 1.59	6 - 12
Number of girls	/	16	/
Number of boys	/	88	/
Only child	/	51	/
Intelligence Quotient	IQ	101.38 ± 11.75	80 - 135
Mean Framewise Displacement	FD	0.13 ± 0.08	0.05 - 0.46
Family income per month (yuan, RMB)			
< 5,000 yuan	/	7	/
5,000 - 10,000 yuan	/	39	/
10,000 -15,000 yuan	/	37	/
> 15,000 yuan	/	21	/
Medication			
Drug-naive	/	55	/
Methylphenidate	/	39	/
Atomoxetine	/	10	/
Swanson, Nolan, and Pelham Rating Scale (SNAP-IV)			
Inattention	SNAP-I	18.44 ± 4.97	6.00 - 27.00
Hyperactivity/Impulsivity	SNAP-HI	14.13 ± 5.93	1.00 - 27.00
Oppositional Defiant Disorder	SNAP-ODD	12.22 ± 5.82	1.00 - 24.00
Strengths and Difficulties Questionnaire (SDQ)			
Emotional Symptoms	SDQ-ES	3.25 ± 2.24	0.00 - 9.00
Conduct Problems	SDQ-CP	2.98 ± 1.90	0.00 - 8.00
Inattention-Hyperactivity	SDQ-IH	7.59 ± 1.83	3.00 - 10.00
Peer Problems	SDQ-PP	3.27 ± 2.14	0.00 - 10.00
Prosocial Behaviour	SDQ-PB	6.73 ± 1.94	2.00 - 10.00
Behavior Rating Inventory of Executive Function, Second Edition (BRIEF-2)			
Inhibition	BRIEF-IB	15.79 ± 3.28	9.00 - 22.00
Self-Monitor	BRIEF-SM	9.29 ± 1.82	5.00 - 12.00

Shift	BRIEF-S	13.82 ± 2.86	8.00 - 21.00
Emotional Control	BRIEF-EC	15.41 ± 3.89	8.00 - 24.00
Initiative	BRIEF-IA	10.47 ± 2.22	5.00 - 15.00
Working Memory	BRIEF-WM	17.85 ± 3.27	10.00 - 24.00
Plan/Organize	BRIEF-PO	17.59 ± 3.03	9.00 - 24.00
Task-Monitor	BRIEF-TM	13.16 ± 1.95	8.00 - 15.00
Organization of Materials	BRIEF-OM	12.36 ± 3.13	6.00 - 18.00
Test of Variables of Attention (TOVA)			
Omission Errors	TOVA-OE	0.17 ± 0.15	0.00 - 0.76
Commission Errors	TOVA-CE	0.09 ± 0.08	0.01 - 0.59
Intrasubject Variability	TOVA-IV	120.76 ± 47.33	16.66 - 282.63
Response Sensitivity Score	D’	2.66 ± 0.92	0.86 - 4.79
Go/No-Go task (GNG)			
Omission Errors	GNG-OE	5.58 ± 4.30	0.00 - 21.00
Commission Errors	GNG-CE	6.24 ± 8.58	0.00 - 45.00
Intrasubject Variability	GNG-IV	150.23 ± 46.45	67.66 - 285.80
Simon task			
Congruent Accuracy	Simon-CACC	0.84 ± 0.12	0.40 - 1.00
Congruent Intrasubject Variability	Simon-CIV	154.51 ± 47.08	71.17 - 320.48
Incongruent Accuracy	Simon-IACC	0.75 ± 0.18	0.10 - 1.00
Incongruent Intrasubject Variability	Simon-IIV	151.83 ± 50.17	77.07 - 284.61
Simon Effect	Simon-SE	0.09 ± 0.14	-0.25 - 0.55
1-back task			
Accuracy	1-back-ACC	0.65 ± 0.19	0.05 - 1.00
Intrasubject Variability	1-back-IV	346.07 ± 163.96	0.00 - 652.23
Iowa Gambling Task (IGT)			
Net Score	IGT-NS	1.00 ± 23.11	-78.00 - 48.00
Balloon Analog Risk Task (BART)			
Earning	BART-E	222.60 ± 98.08	48.00 - 456.00

Explosion Number	BART-EN	6.00 ± 4.25	0.00 - 20.00
Adjusted Pumps	BART-AP	10.24 ± 6.07	1.60 - 26.43

Figures

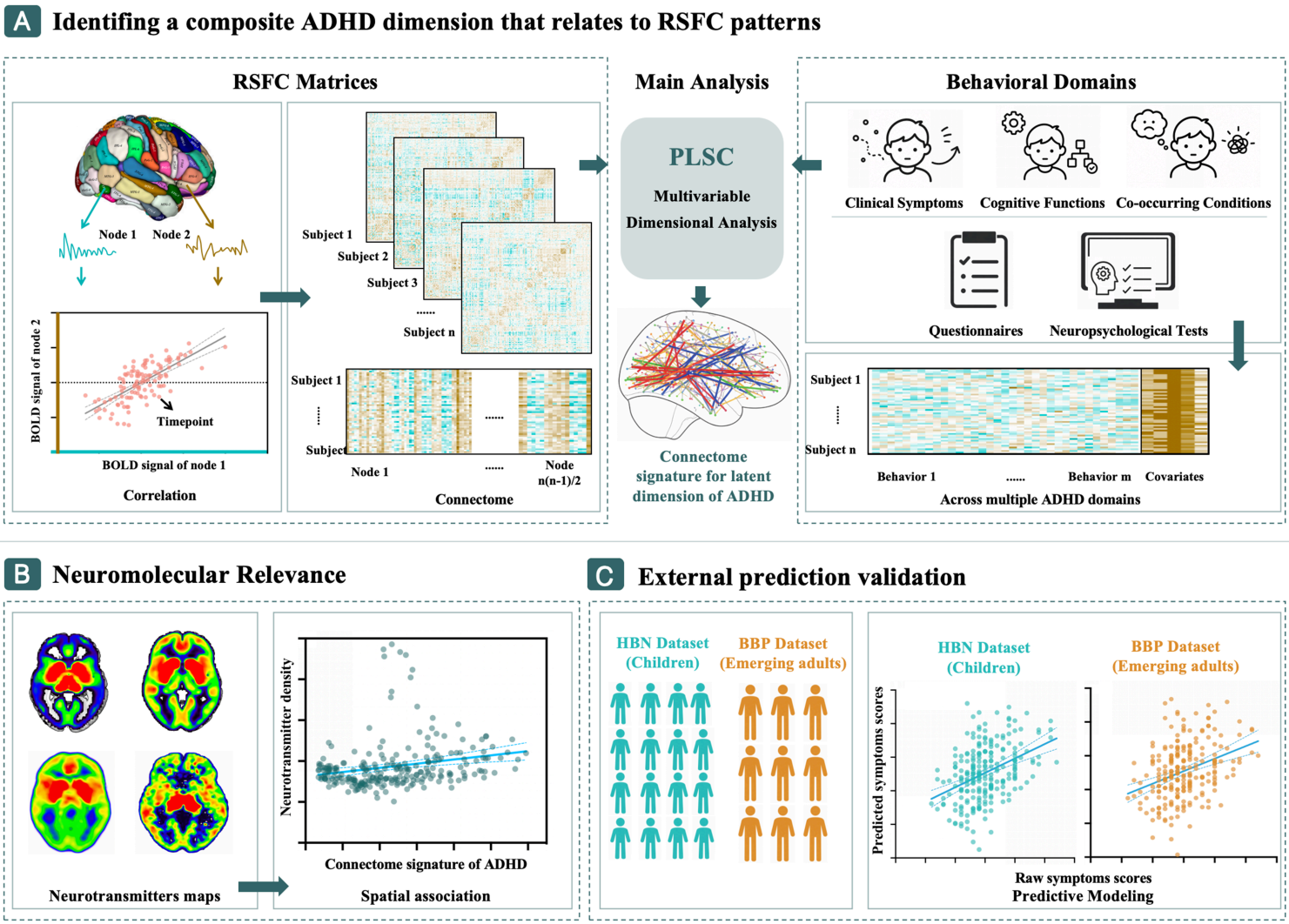


Figure 1

Overview of data analysis processes. **Panel A**: The input to PLSC consists of a whole-brain connectome matrix and a behavior matrix. Each edge in the connectome matrix represents the Pearson correlation coefficient between the BOLD signal time series of two nodes. To reduce computation, the upper triangle and diagonal values are excluded, and the RSFC matrix for each subject is reshaped into a single row, resulting in a connectome matrix for input. The behavior matrix includes core ADHD symptoms, cognitive functions, and co-occurring conditions. These two matrices are then input into the PLSC algorithm to extract a composite ADHD dimension related to RSFC patterns. **Panel B**: Investigating the neuromolecular relevance of brain connectomes underlying interindividual differences in ADHD. **Panel C**:

Assessing whether the ADHD-related brain connectome can predict ADHD symptoms in two independent datasets.

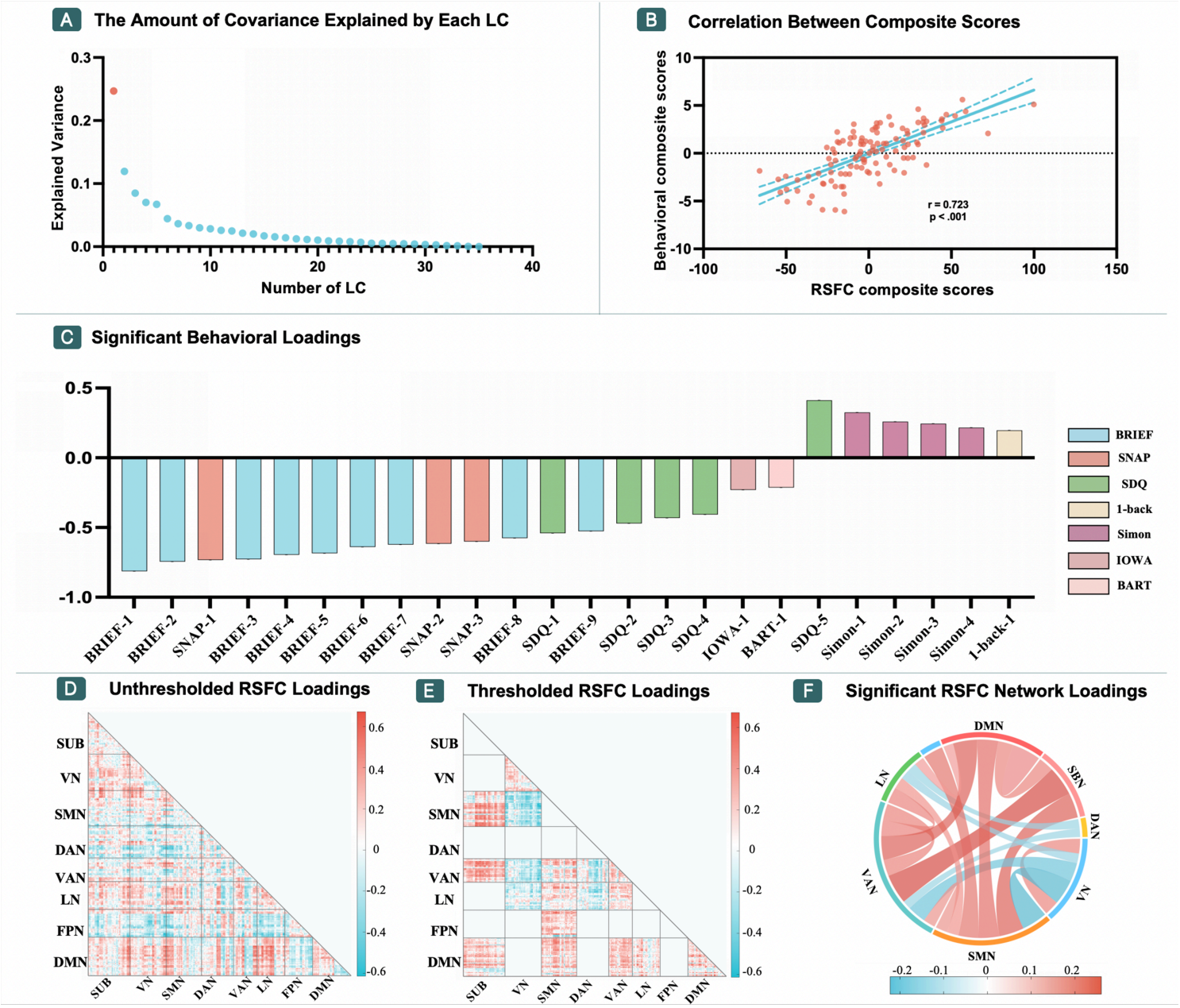


Figure 2

PLSC identifies a robust latent component linking ADHD and RSFC in the discovery dataset. **Panel A**: Covariance explained by each latent component (LC). Only LC1 survived permutation testing with FDR correction ($q < 0.05$), accounting for 24.7% of RSFC–behavior covariance. **Panel B**: Scatter plot showing the significant association between individual RSFC and behavioral composite scores for LC1 ($r = 0.723$, $p < 0.001$, Pearson correlation). **Panel C**: Group-level correlations between participants' behavioral measures and their composite scores, highlighting the 24 strongest associations. **Panel D**: Unthresholded correlations between RSFC and RSFC composite scores, with yellow and blue indicating positive and negative associations with LC1, respectively. **Panel E**: Thresholded correlations showing

only within- or between-network blocks with significant bootstrapped Z scores (FDR q < 0.05). **Panel F**: Network-averaged correlations of RSFC and RSFC composite scores for significant blocks.
Abbreviations: BRIEF, Behavior Rating Inventory of Executive Function; SNAP, Swanson, Nolan, and Pelham Rating Scale; SDQ, Strengths and Difficulties Questionnaire; IGT, Iowa Gambling Task; BART, Balloon Analog Risk Task; SBN, subcortical network; VN, visual network; SMN, somatomotor network; DAN, dorsal attention network; VAN, ventral attention network; LN, limbic network; FPN, frontoparietal network; DMN, default mode network.

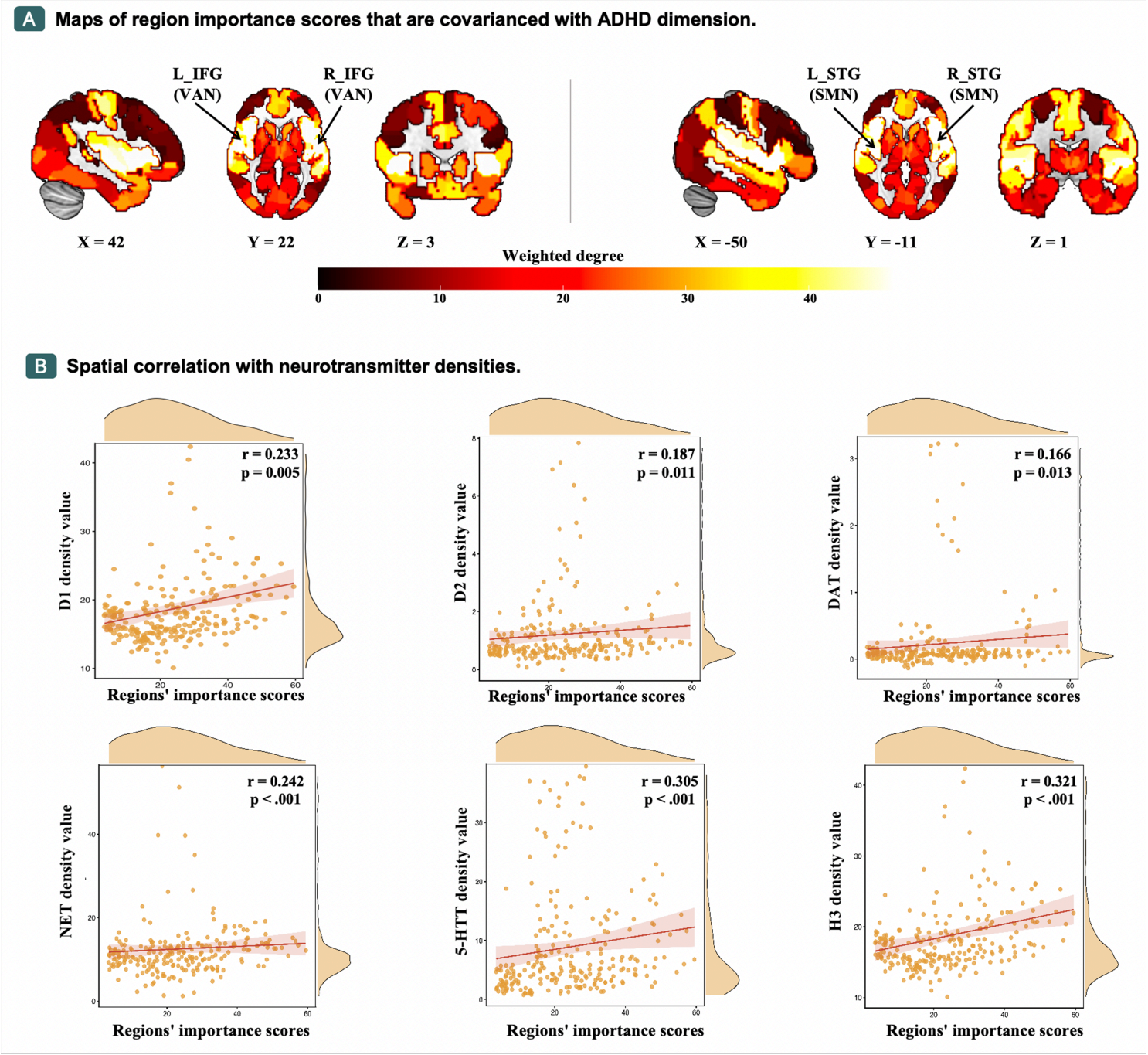


Figure 3

Panel A: Maps of region importance scores associated with the ADHD dimension. RSFC loadings were summed for each region of the Brainconnectome atlas to derive the region importance scores. **Panel B:** Spatial correlations with neurotransmitter densities. RSFC loadings were correlated with the distribution of neurotransmitter systems implicated in ADHD using Pearson correlation analysis. Significant correlations were found between region importance scores and the densities of D1 (r = 0.233, p = 0.005), D2 (r = 0.187, p = 0.011), DAT (r = 0.166, p = 0.013), NET (r = 0.242, p < 0.001), 5-HTT (r = 0.305, p < 0.001), and H3 (r = 0.321, p < 0.001). **Abbreviations**: L_IFG, left inferior frontal gyrus; R_IFG, right inferior frontal gyrus; VAN, ventral attention network; L_STG, left superior temporal gyrus; R_STG, right superior temporal gyrus; SMN, somatomotor network.

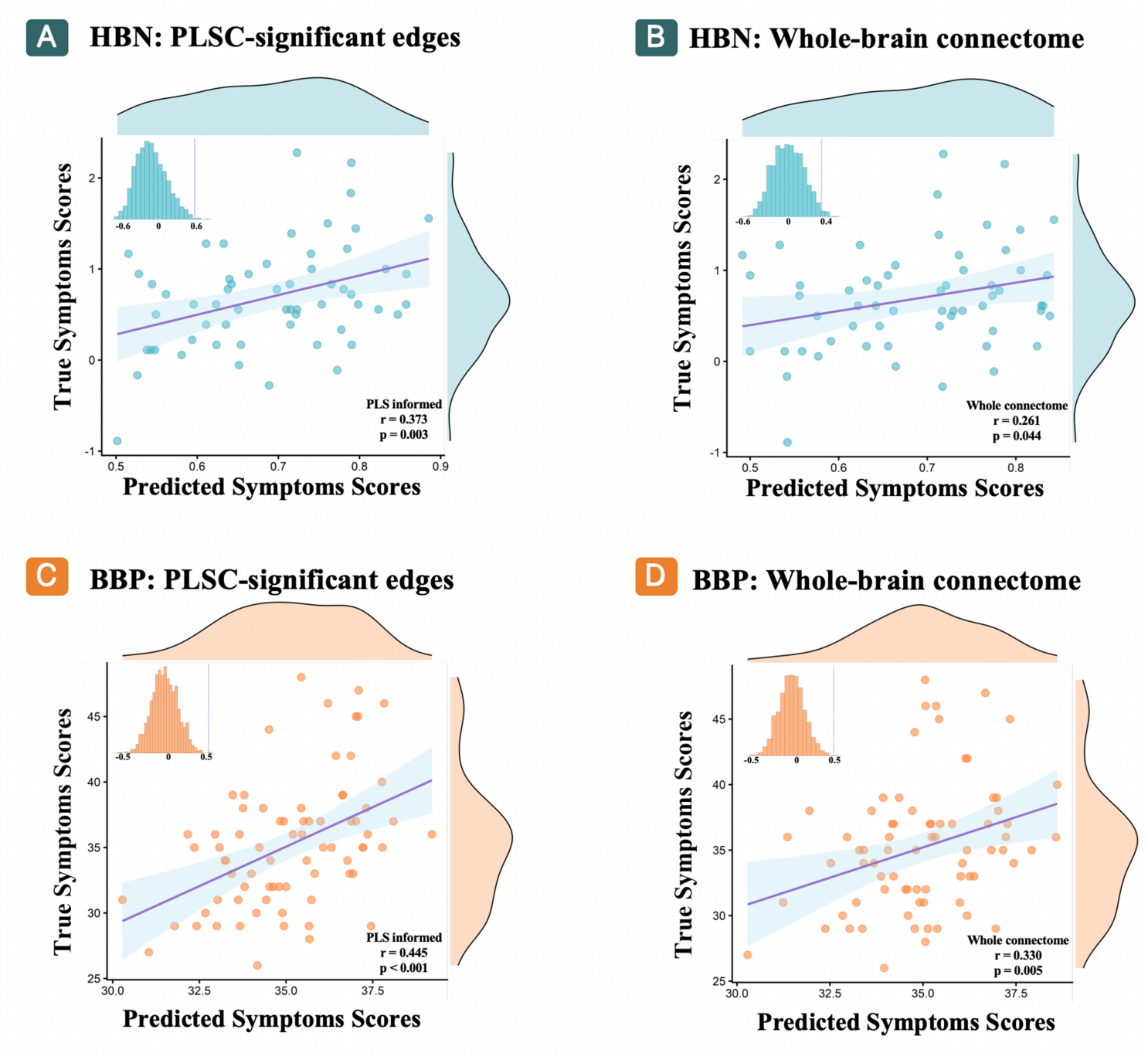


Figure 4

External validation of RSFC-based prediction models for ADHD symptom scores. **Panels A and B** show the predictive performance in the HBN dataset. ADHD symptom scores were predicted using either significant RSFC edges derived from the PLSC spatial pattern identified in the discovery dataset (panel A; $r = 0.373$, $p = 0.003$, permutation $p = 0.003$) or the whole-brain connectome (panel B; $r = 0.261$, $p = 0.044$, permutation $p = 0.016$). **Panels C and D** show the predictive performance in the BBP dataset. Significant prediction was observed using both the PLSC-derived significant RSFC edges (panel C; $r = 0.445$, $p < 0.001$, permutation $p = 0.001$) and the whole-brain connectome (panel D; $r = 0.330$, $p = 0.005$, permutation $p < 0.001$). Prediction performance was evaluated using Pearson correlations between observed and predicted symptom scores, with predicted scores averaged across 100 repetitions of five-fold cross-validation.

Supplementary Files

This is a list of supplementary files associated with this preprint. Click to download.

- SupplementaryMaterials4.docx